David Runt; Jaroslav Novotný; Jan Pruška

Mathematical modelling of rock bolt reinforcement

In: Jan Chleboun and Pavel Kůs and Petr Přikryl and Karel Segeth and Jakub Šístek and Tomáš Vejchodský (eds.): Programs and Algorithms of Numerical Mathematics, Proceedings of Seminar. Janov nad Nisou, June 19-24, 2016. Institute of Mathematics CAS, Prague, 2017. pp. 102–111.

Persistent URL: http://dml.cz/dmlcz/703004

Programs and Algorithms of Numerical Mathematics 18
J. Chleboun, P. Kůs, P. Přikryl, K. Segeth, J. Šístek, T. Vejchodský (Eds.)
Institute of Mathematics CAS, Prague 2017

MATHEMATICAL MODELLING OF ROCK BOLT REINFORCEMENT

David Runt, Jaroslav Novotný, Jan Pruška

Faculty of Civil Engineering, Czech Technical University in Prague
Thákurova 7, 166 29 Prague 6, Czech Republic
david.runt@fsv.cvut.cz, jaroslav.novotny@fsv.cvut.cz, Pruska@fsv.cvut.cz

Abstract: Rock bolts as construction elements are often used in underground civil engineering projects. This work deals with their numerical modelling. Aydan special finite elements for the description of rock bolts and hexahedral quadratic finite elements for the description of rock massif were used. A code for the computation of stiffness matrices and right hand sides of these elements was developed. The code was tested on several simple test examples and their results were compared with the analytical solution. Stresses in a rock massif in the surrounding of an excavation reinforced by rock bolts were computed. The results show that the use of rock bolts can reduce the areas of maximal mechanical stress in the vicinity of excavations.

Keywords: rock bolt reinforcement, mathematical modelling, the finite element method

MSC: 65N30, 74B05, 74G15, 74L10

1. Introduction

Rock bolts as reinforcing construction elements are often used in underground civil engineering projects (Fig. 1).

Several special finite elements for rock bolt modelling were developed. The most widely used element was presented by Aydan [1]. The so-called Aydan element consists of two groups of nodes. The first group represents a rod sub-element, which is a simple model of a steel bar. The remaining nodes are located on the interface of cement grout and rock massif. The connection of the bar with the surrounding rock by cement grout is represented by the joint action of both groups of nodes. This paper is focused on the six-node type of the Aydan element with quadratic shape functions, which is used in 3D models.

The computation of the stiffness matrix of this element and its application in the 3D model of two tunnels reinforced by rock bolts is described. The rock bolts

DOI: 10.21136/panm.2016.13

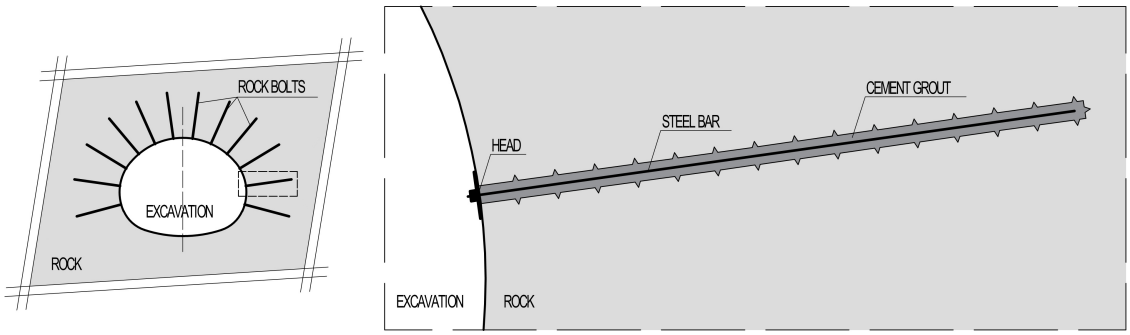

Figure 1: Rock bolts.

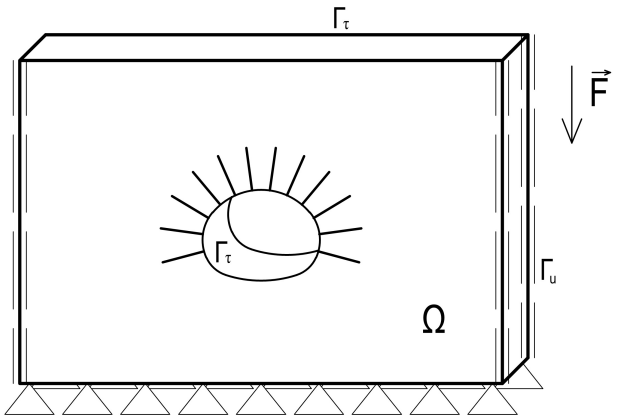

Figure 2: Classical formulation of the linear elasticity problem.

are fastened by cement grout along their full length. The geometry of the model corresponds to the characteristic cross section of the Brusnice tunnel that is a part of the Blanka tunnel complex, an underground part of the Prague City Ring Road.

2. Classical formulation of a linear elasticity problem

Differential equations describe real physical processes inside the material. The classical formulation of the linear elasticity problem is described in [3], for instance.

We consider a linear elastic body that occupies a domain Ω (Fig. 2). We look for the vector of displacements $\mathbf{u} = (u_1, u_2, u_3)$ satisfying Lamé equations in the domain Ω, see Equations (1),

$$(\lambda + \mu) \sum_{j=1}^{3} \frac{\partial^2 u_j}{\partial x_i \partial x_j} + \sum_{j=1}^{3} \frac{\partial^2 u_i}{\partial x_j^2} + F_i = 0, \quad i = 1, 2, 3 \tag{1}$$

where λ, μ are the Lamé coefficients, x_i and F_i stand for the i-th coordinate com-

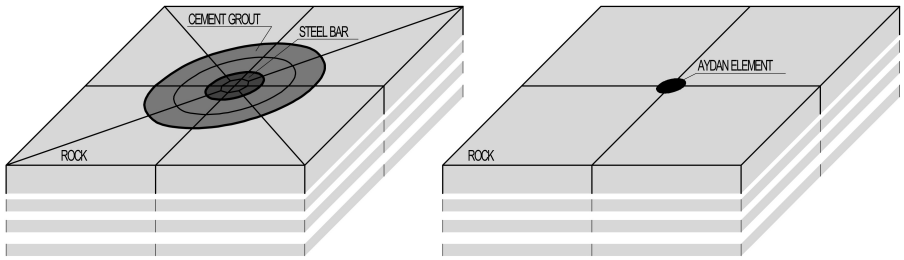

Figure 3: Finite element discretization of the rock bolt reinforcement without and with a special rock bolt element.

ponent and volumetric load component, respectively. Displacements are prescribed on Γ_u and the stress vector is given on Γ_τ (see Fig. 2), that is,

$$u_i = 0, \quad i = 1, 2, 3 \text{ on } \Gamma_u \tag{2}$$

$$\sum_{j=1}^{3} \tau_{ij}\nu_j = 0, \quad i = 1, 2, 3 \text{ on } \Gamma_\tau \tag{3}$$

where $\tau = (\tau_{ij})$ is the stress tensor and $\nu = (\nu_1, \nu_2, \nu_3)$ is the outward unit normal vector to the boundary of Ω.

We prescribed zero displacements on the bottom, on the sides and on the front and back faces of the domain Ω, see Equation (2). The zero stress vector is prescribed on the excavation surface and on the top surface of the body Ω, see Equation (3).

3. The finite element method

3.1. Rock bolt element of the Aydan type

Because a detailed discretization of the rock bolt reinforcement including the steel bar and fastening material needs a generation of a complicated finite element mesh, special finite elements were derived, see Fig. 3.

The Aydan rock bolt element with quadratic shape functions has six nodes (Fig. 4). Three of them represent the steel rod (nodes 1, 2 and 3). The others are located on the interface between the fastening material and the surrounding rock. The rock bolt element is connected to the elements, which represent rock massif, by nodes 4, 5 and 6 (Fig. 4). The connection of the bar with surrounding rock massif by cement grout is represented by the joint action of both groups of the nodes.

Several simplifications were considered during the derivation of the stiffness matrix of the Aydan element. The steel rod and body formed by the fastening material are assumed axially symmetric and coaxial bodies. Both mentioned materials are considered homogeneous, isotropic and linear elastic. Therefore the dependence between stresses and deformations of these materials is described by linear Hooke's law. The radius of the rock bolt is negligible with respect to its length. Therefore, nodes 1 and 4 have identical coordinates. The same is valid for nodes 2 and 5 or 3

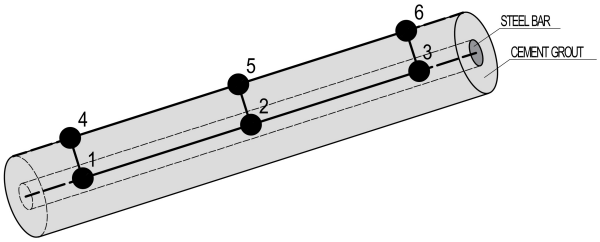

Figure 4: Aydan six-node rock bolt element.

and 6. However, the assumption of negligible radius cannot be applied to the process of derivation of the stiffness matrix. Only three types of deformations of the Aydan element are included in the computation:

- relative longitudinal deformation of the steel bar caused by different axial displacements of nodes 1, 2 and 3,
- relative cross shear deformation of the steel bar caused by different radial displacements of nodes 1, 2 and 3,
- relative longitudinal shear deformation of fastening material caused by different axial displacements of nodes 1, 2 and 3 with respect to nodes 4, 5 and 6,
- relative cross deformation of fastening material caused by different radial displacements of nodes 1, 2 and 3 with respect to nodes 4, 5 and 6,

To define the element stiffness matrix, we introduce matrices $\mathbf{D}$ and $\mathbf{B}$. In detail,

$$\mathbf{D} = \begin{bmatrix} E^t & 0 & 0 & 0 & 0 & 0 \\ 0 & G^t & 0 & 0 & 0 & 0 \\ 0 & 0 & G^t & 0 & 0 & 0 \\ 0 & 0 & 0 & G^z & 0 & 0 \\ 0 & 0 & 0 & 0 & D^z & 0 \\ 0 & 0 & 0 & 0 & 0 & D^z \end{bmatrix}.$$

Here, E^t is Young's modulus of steel, G^t and G^Z is the shear modulus of steel and fastening material, D^Z is Young's modulus of the fastening material multiplied by two. The multiplicative factor of two reflects the effects of enlacement of the cement grout by the rock massif.

Next,

$$\mathbf{B} = \begin{bmatrix} \mathbf{B}_1 & \mathbf{B}_2 \\ \mathbf{B}_3 & -\mathbf{B}_3 \end{bmatrix},$$

where

$$\mathbf{B}_1 = \begin{bmatrix} N_1' & 0 & 0 & N_2' & 0 & 0 & N_3' & 0 & 0 \\ 0 & N_1' & 0 & 0 & N_2' & 0 & 0 & N_3' & 0 \\ 0 & 0 & N_1' & 0 & 0 & N_2' & 0 & 0 & N_3' \end{bmatrix},$$

$$\mathbf{B}_3 = \begin{bmatrix} cN_1 & 0 & 0 & cN_2 & 0 & 0 & cN_3 & 0 & 0 \\ 0 & N_1 & 0 & 0 & N_2 & 0 & 0 & N_3 & 0 \\ 0 & 0 & N_1 & 0 & 0 & N_2 & 0 & 0 & N_3 \end{bmatrix},$$

B_2 is a zero matrix, the prime denotes the derivative with respect to ξ (see (4)), and $c = 2/((r^h + r^t)l$, where $l = \ln(r^h/r^t)$ and $r^t,\ r^h$ are the respective diameters of the steel bar and the rock bolt borehole, the latter is equivalent to the diameter of the body formed by the fastening material.

The constant c was derived in [1]. Shape functions are quadratic:

$$\begin{aligned} N_1 &= 0.5 \cdot \xi \cdot (\xi - 1), \\ N_2 &= 1 - \xi^2, \\ N_3 &= 0.5 \cdot \xi \cdot (\xi + 1), \end{aligned} \tag{4}$$

where $\xi \in [-1; 1]$ is the local coordinate. The stiffness matrix of the rock bolt referential element is

$$\mathbf{K} = \int_{-1}^{1} \mathbf{B}^T \mathbf{D} \mathbf{B} \, \mathrm{d}\xi,$$

where $\mathbf{B}^T =$ is the transpose of $\mathbf{B}$.

Constant values of the displacements across the cross section of the rock bolt are considered. Therefore, the volume integral is reduced to one-dimensional integral with the integration area of the length of the rock bolt element. Three-point Gaussian numerical integration was used for the calculation of the one-dimensional integral.

Finally, it is necessary to transform the stiffness matrix from local to global system of coordinates.

3.2. Hexahedron - rock element for 3D model

Rock massif is represented by hexahedral elements with 20 nodes [2] in 3D model. Eight nodes are located in vertices, remaining twelve are located in the centres of edges. Gaussian numerical integration of third order was used for calculating stiffness matrices and right hand sides.

4. Test example and comparison with analytical solution

An analytical expression for stresses in excavation is known only for several simple cases. For a circular excavation without rock bolts, such solution is described in [6]. For a circular excavation with rock bolts, an analytical solution is known only if an

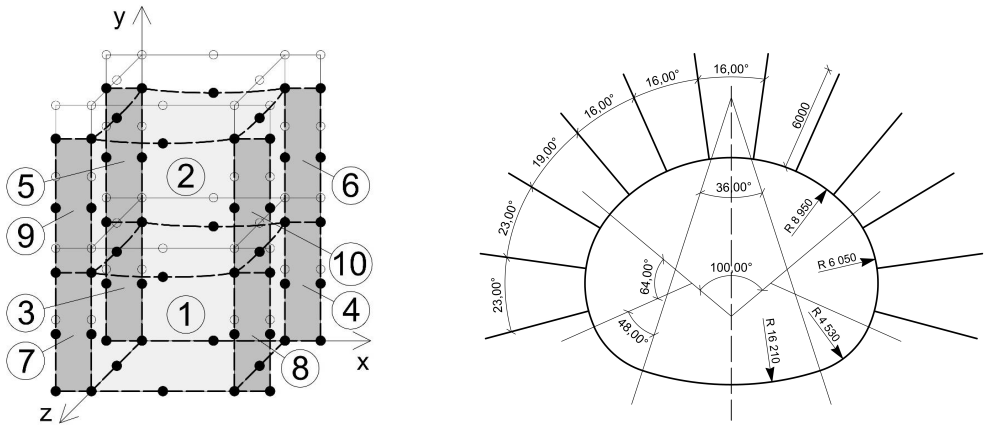

Figure 5: Test example consisting of two bricks and eight Aydan elements (left), and shape of excavation and spacing of rock bolts (right).

averaging of the rock bolt and rock material properties is introduced, see [4]. Therefore we studied several simple problems where the analytical solution can easily be derived. One of the simple problems used for the verification of our implementation of the Aydan rock bolt element is presented below, see Fig. 5.

This example consists of two bricks (elements 1 and 2) of $1 \times 2 \times 1$ m reinforced by eight Aydan elements (elements 3 - 10). Zero displacements are prescribed at the base of the body, the other displacements are restricted to the $y-$direction. The following material properties and loads were considered:

$$\begin{aligned} E_{rock} &= 500 \text{ MPa}, \ \nu_{rock} = 0.2, \\ E_{steel} &= 210 \text{ GPa}, \ \nu_{steel} = 0.3, \\ E_{grout} &= 30 \text{ GPa}, \ \nu_{grout} = 0.2, \ f_y = -25 \text{ kN} \cdot \text{m}^{-3}. \end{aligned}$$

Analytical solution was easy to compute from the equation

$$\frac{d}{dy}\left(EA\frac{du}{dy}\right) + f_y = 0,$$

where A denotes the area of the cross-section. The stiffness of the cross-section was defined by the sum of stiffnesses of the rock bolts and the rock. Results for both numerical and analytical solution are summarized in Table 1. The shape of the deformed body is also depicted in Figure 5.

5. Model of rock bolt reinforcement

The geometry of the model corresponds to the characteristic cross section of the two-tube Brusnice tunnel, which is a part of the Blanka tunnel complex. Two three lane motorways are situated inside of these two tunnels. All data necessary for the model creation were taken from [7].

Solution	Displacement of rock at y = 1 m	Displacement of rock at y = 2 m
Numerical	from -0.341×10^{-4} to -0.402×10^{-4} m	from -0.468×10^{-4} to -0.532×10^{-4} m
Analytical	-0.383×10^{-4} m	-0.511×10^{-4} m

Table 1: Comparison of numerical and analytical solution at $y = 1$ and $y = 2$ m.

5.1. Input data

Each of the two excavations is composed of four types of circular arcs, has a height of 12.8 metres, a width of 16.6 metres, and an area of almost 180.0 square metres. Twelve rock bolts six metres long are placed in the tunnel arch. The angle between two adjacent rock bolts varies from 18° to 23° (Fig. 5 right).

The distance between parallel planes containing rock bolt bundles in the direction of the axis of the tunnel is 1.25 m. All 24 rock bolts are located in the central plane of the model. Therefore, thickness of the model periodic segment is considered also 1.25 m. Each rock bolt is, in fact, a steel bar with a radius of 2.0 cm that is fastened by cement grout along its full length in the borehole with a diameter of 6.0 cm.

The width of the whole model is 150.0 metres and the height varies from 51.4 metres up to 62.6 metres. The thickness of a rock cover is 13.3 metres for the left excavation and 12.8 metres for the right one (Fig. 6 top). For this model we consider boundary conditions that were already described in the classical formulation of the problem. The rock massif is formed by mildly eroded slates, which are very common in the surrounding of the tunnel. Steel and cement grout are another materials contained in the model. It is necessary to prescribe Young's modulus, Poisson's ratio and specific density for all the materials,

$$\begin{aligned} E_{rock} &= 400 \text{ MPa}, \ \nu_{rock} = 0.28, \ \rho_{rock} = 2450 \text{ kg} \cdot \text{m}^{-3}, \\ E_{steel} &= 210 \text{ GPa}, \ \nu_{steel} = 0.3, \\ E_{grout} &= 30 \text{ GPa}, \ \nu_{grout} = 0.2. \end{aligned}$$

In the development of the finite element mesh, a circular zone around the excavation was created in order to properly couple the Aydan elements with the brick elements (Fig. 6 bottom). The mesh consists of 61,368 hexahedrons and 360 rock bolt elements and it is represented by 297,931 nodes. The mesh is composed of four layers of elements with the same thickness in the direction of the axis of the tunnel.

5.2. Results

We considered two studies. In the first case, we assumed the excavations without any rock bolts. Then the model with rock bolts was used. An influence of rock bolts is recognizable only in the close vicinity of the excavations, therefore we analyse the results only in this detailed area, especially in the surrounding of the left excavation. Stress σ_{yy} in the vertical direction and stress σ_{xx} in the horizontal direction is depicted (Fig. 7). The influence of rock bolts is most evident, if the

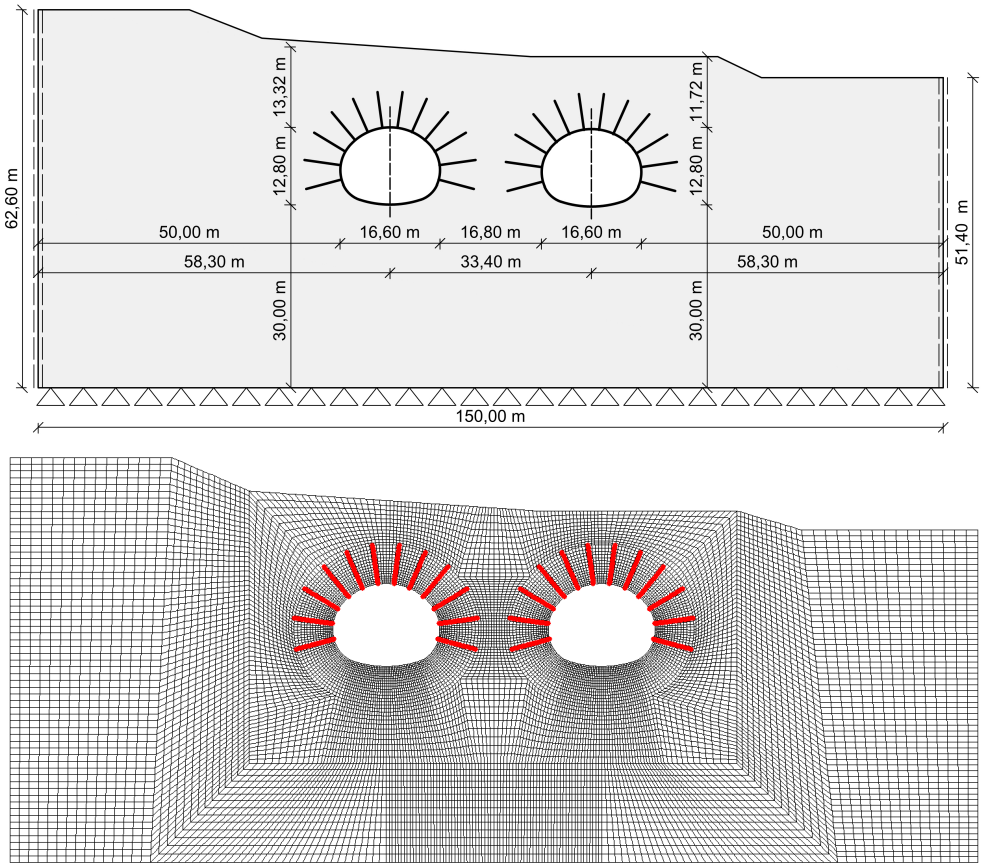

Figure 6: Geometry of the whole model (top), and finite element mesh including the position of rock bolts (bottom).

direction of their axis is similar to the direction of the considered stress. Areas with large stress are redistributed into several smaller areas, although the stress need not decrease (Fig. 8).

Rock bolts placed above the excavation have greater impact on the vertical stress and rock bolts placed on the sides have greater impact on the horizontal stress. Stresses in the area above the excavation are relatively low, so rock bolts cannot achieve full activation here. Presence of rock bolts is most evident in the horizontal stress and mainly on the sides of the excavations (Fig. 9). The location of the rock bolts is clearly apparent from the local stress anomalies.

6. Conclusion

The influence of rock bolts is recognizable from our results. Rock bolts reduce local extreme values of stresses. In general, they mildly raise stresses in the radial direction and they help to create rock arch and improve the stability of the excavation. When using rock bolts, areas with large stress are redistributed into several

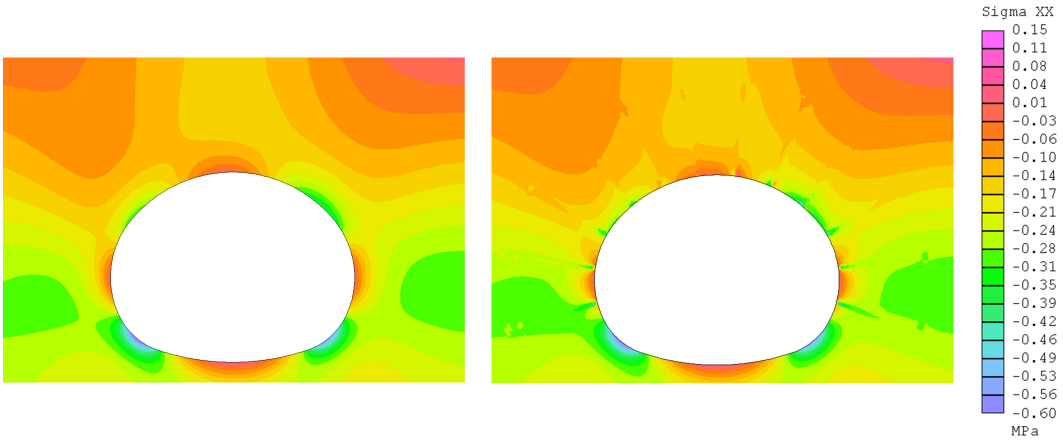

Figure 7: Stress σ_{xx} in the surrounding of the left excavation without rock bolts (left) and with rock bolts (right).

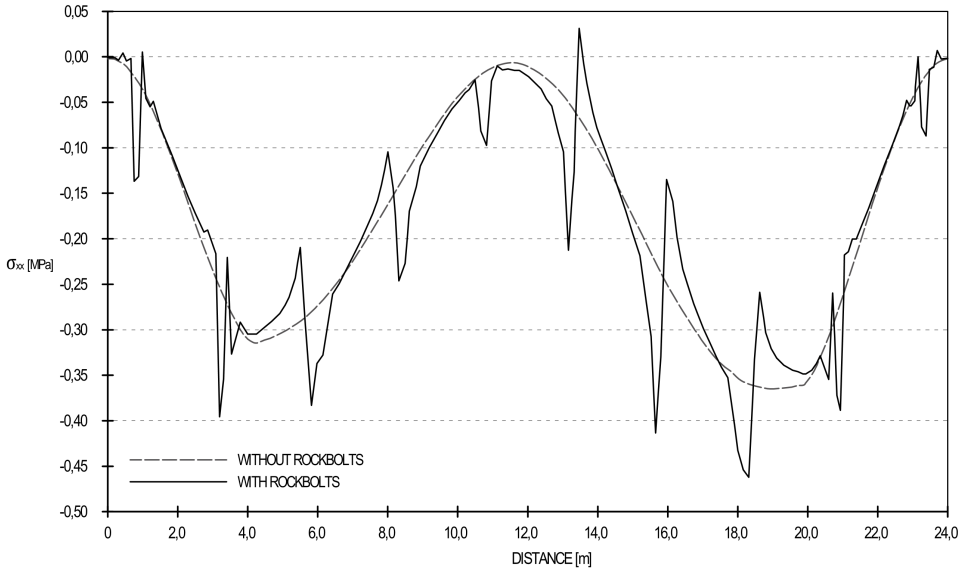

Figure 8: Stress σ_{xx} along the upper part of the excavation arc – without rock bolts (dashed line) and with rock bolts (solid line).

smaller areas, although the stress need not decrease. Described influence corresponds to theoretical knowledge of the functioning of rock bolt reinforcement. It is possible to combine special rock bolt elements with other types of elements with appropriate shape functions and this is the way how to create complex numerical models of reinforced excavations. Due to the simplicity of the rock bolt element it is quite easy to create its different modifications with various shape functions. These modifications were described by Aydan [1], Chao [5] or Runt [8]. The resulting elements can be used in both 2D and 3D models.

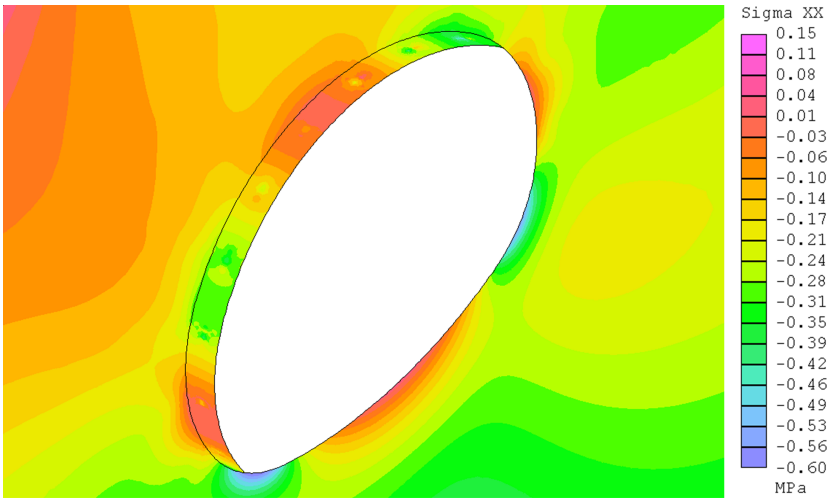

Figure 9: Stress σ_{xx} inside the excavation.

Acknowledgements

This work was supported by the grant project SGS16/004/OHK1/1T/11 provided by Czech Technical University in Prague, Faculty of Civil Engineering.

References

[1] Aydan, O.: *The stabilisation of rock engineering structures by rockbolts*. Nagoya University, Nagoya, 1989.

[2] Bathe, K. J.: *Finite element procedures*. Prentice-Hall, New Jersey, 1996.

[3] Brdička, M.: *Continuum mechanics*. Czechoslovak Academy of Sciences, Prague, 1959 (in Czech).

[4] Carranza-Torres, C.: Analytical and numerical study of the mechanics of rock-bolt reinforcement around tunnels in rock masses. Rock. Mech. Rock. Engng. **42** (2009), 175–228.

[5] Chao, T.: *The numerical modelling of rockbolts in geomechanics by finite element methods*. Ph.D. thesis, Brunel University, London, 1998.

[6] Jaeger, J. C., Cook N. G. W.: *Fundamentals of rock mechanics*. Chapman and Hall, London, 1979.

[7] Nosek, J.: *Evaluation of reliability of structural analyses of tunnels in the Czech Republic on the bases of analyses of the monitoring results*. Ph.D. thesis, Czech Technical University in Prague, Prague, 2015 (in Czech).

[8] Runt, D.: *Rock bolt element in the finite element method*. M.Sc. thesis, Czech Technical University in Prague, Prague, 2016 (in Czech).